ACS Macro Letters

Letter

pubs.acs.org/macroletters

Magnetic Field Alignment of a Diblock Copolymer Using a Supramolecular Route

Manesh Gopinadhan,[†] Pawel W. Majewski,[†] Evan S. Beach,[‡] and Chinedum O. Osuji*[,†]

[†]Department of Chemical and Environmental Engineering and [‡]Department of Chemistry, Yale University, New Haven, Connecticut 06511, United States

Supporting Information

ABSTRACT: Large-area uniform magnetic alignment of a self-assembled diblock copolymer has been achieved by the selective sequestration of rigid moieties with anisotropic diamagnetic susceptibility within one block of the system. The species is based on a biphenyl core and is confined in the acrylic acid domains of a poly(styrene-*b*-acrylic acid) block copolymer by hydrogen bonding between an imidazole headgroup and the acrylic acid units. Microphase separation produces hierarchically ordered systems of smectic layers within lamellae and smectic layers in the matrix surrounding hexagonally packed poly(styrene) cylinders, as a function of imidazole/acrylic acid stoichiometry. The magnetic field aligns the smectic layers as well as the block copolymer superstructure in a manner dependent on the anchoring condition of the biphenyl species at the block copolymer interface. Surprisingly, this is found to depend on the composition of the system. This approach is synergistic with recent efforts to engineer functional supramolecular block copolymer assemblies based on rigid chromophores. It offers a facile route to large area control of microstructure as required for full exploitation of functional properties in these systems.

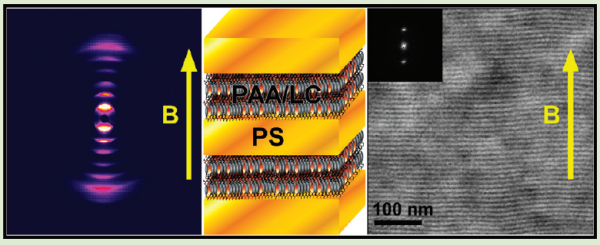

Noncovalent interactions provide a flexible means of engineering new chemical entities with tailored properties.[1,2] The formation of supramolecular species by noncovalent attachment of small molecules to a polymer backbone has been exploited to develop a range of functional materials.[3−6] Ionic conductors based on charge transfer complexes of poly(4-vinyl pyridine) with methane sulfonic acid[7] and electrical conductors based on poly(aniline)[8] have been realized in self-organized supramolecular homopolymers. Functional block copolymers with stimuli-responsive photonic band gaps,[9,10] semiconducting materials based on hydrogen bonding of a quaterthiophene derivative with poly(styrene-*b*-4-vinyl pyridine),[11] bicontinuous donor/acceptor networks in semiconducting rod−coil systems with noncovalently attached nanomaterials,[12] and supramolecular composite block polymer films for electrical switching[13] have also been demonstrated. A full exploitation of such promising functional properties requires effective control of nanostructure, for example, to uniquely define the fast electron or hole conduction direction in electro-optically active systems or to precisely control the orientation of optical axes in photonic materials. However, the development of globally well aligned morphologies in these systems remains a persistent challenge, as it is also in nonfunctionalized block copolymers.[14] While the use of secondary bonding to introduce physicochemical functionality is well documented, as we demonstrate here, the potential also exists to deliberately use nonbonded interactions to enable facile alignment of hierarchical self-assembled morphologies in block copolymer systems. We show that hydrogen bonding between a rigid biphenyl species and one block of a diblock copolymer can be used to render the system susceptible to strong alignment by magnetic fields in a composition dependent manner. At low stoichiometries, an immobile smectic mesophase within a lamellar superstructure was produced which displayed no alignment. At intermediate stoichiometries, the same lamellar-in-lamellar motif was well aligned by application of the field during cooling from the disordered melt. At high stoichiometries, the system transitioned to a hexagonally packed cylinder phase with a smectic substructure and showed strong alignment under the influence of the field. Surprisingly, the transition from lamellar to cylinder morphology was attended by a transition from a homeotropic to a planar anchoring of the biphenyl ligand at the intermaterial dividing surface (IMDS). This supramolecular approach provides a convenient and tunable method for the large area alignment of block copolymers using magnetic fields. Further, it is synergistic with recent efforts in the engineering of supramolecular organic semiconductors[15] and nonlinear optical polymers.[16] Chromophore rigidity can provide both the enhanced conjugation lengths that dictate optical absorption as well as the magnetic anisotropy and orientational order that enable facile alignment by magnetic fields.

Magnetic field directed self-assembly relies on the presence of anisotropy in the magnetic susceptibility such that a significant free energy difference with respect to k_BT exists

Received: October 3, 2011
Accepted: December 7, 2011
Published: December 14, 2011

   dx.doi.org/10.1021/mz2001059 | *ACS Macro Lett.* 2012, 1, 184−189

among various orientations of the system in the presence of the field. In typical coil−coil diblock copolymers such as poly(styrene-*b*-isoprene), the anisotropy of susceptibility is a vanishingly small number, with $\nabla\chi$ of the phase separated structure on the order of 10^{-9}, and as a result, magnetic field alignment of these systems does not proceed at any reasonable field strengths.[17] The presence of rigid aromatic moieties significantly enhances the anisotropy of susceptibility with $\nabla\chi \sim 10^{-5}$ possible for biphenyl species.[18,19] Despite the fact that such anisotropy is purely diamagnetic in origin, alignment may proceed at accessible field strengths of a few tesla in systems with grain sizes on the order of 100 nm and larger.[17,20−24] Here, we have utilized hydrogen bonding interactions to selectively sequester a biphenyl moiety within one block of a coil−coil diblock copolymer. The resulting diamagnetic anisotropy of the self-assembled structure provides the required driving force for strong texturing under a magnetic field.

The concept is illustrated schematically in Figure 1a. A supramolecular complex is formed via noncovalent interaction

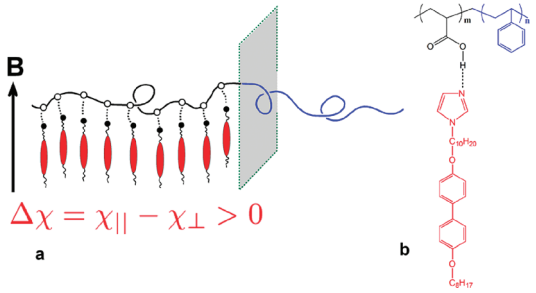

Figure 1. (a) Magnetic field alignment of a supramolecular LC block copolymer occurs subject to the diamagnetic anisotropy of the ligand (in red), and its orientation at the IMDS (in gray); (b) Chemical structures of the PS(5.1k)-*b*-PAA(3.9k) block copolymer and the H-bonded imidazole mesogen.

of rigid biphenyl species with the polymer backbone. A positive diamagnetic anisotropy leads to the alignment of the molecular long axis of the ligand parallel to the applied magnetic field. The alignment of the block copolymer superstructure is dictated by the thermodynamically prescribed orientation of the ligand with respect to the IMDS, shown in gray. The structure of the poly(styrene-*b*-acrylic acid) (PS-PAA) backbone and the imidazole terminated biphenyl mesogen are shown in Figure 1b. The stoichiometry, *R*, is given by the ratio of the number of biphenyl ligands to the number of acrylic acid binding sites. The neat diblock displays a lamellar morphology with a *d*-spacing of 18 nm. The mesogen is a crystalline solid with a melting temperature of 98 °C. X-ray scattering revealed a monolayer structure with a characteristic length scale of 3.3 nm in the small-angle regime corresponding to the layer spacing. The mesogen-diblock copolymer complex is formed in solution, and films of the resulting supramolecular material are produced on slow solvent removal by evaporation. Hydrogen bonding between the imidazole ligand and the acrylic acid repeat units was confirmed by the emergence of band frequencies centered around 1717−1723 cm^{-1} in FTIR (Supporting Information).[25,26] The formation of the liquid crystalline side chain block copolymer at different stoichiometries was evidenced by the distinct phase behavior of the systems relative to the neat diblock or pure meosogen alone, as shown in DSC data (Supporting Information). The T_g of the PS block did not show any significant change, indicating that the mesogens are effectively sequestered within the PAA block. SAXS, POM, and DSC studies confirmed the formation of a homogeneous mesophase without any macrophase separation over the range of compositions studied.

Figure 2 shows SAXS data for samples with $R \leq 0.4$ both as-cast and after alignment under a 5 T magnetic field. The neat

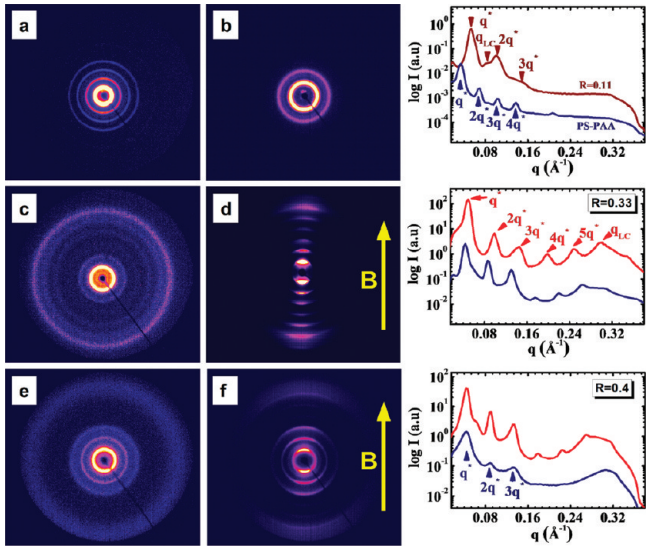

Figure 2. Room temperature 2-D SAXS and corresponding 1D integrated data for (a) neat PS-PAA; (b) $R = 0.11$; (c) $R = 0.33$ (as cast); (d) $R = 0.33$ (after alignment); (e) $R = 0.4$ (as cast); (f) $R = 0.4$ (after alignment). The field direction was vertical with respect to the 2-D data as indicated. Blue and red traces: 1-D data before and after alignment, respectively, for $R = 0.33$ and $R = 0.44$. Data are vertically shifted for clarity.

diblock, $R = 0$, displays a well-ordered lamellar morphology with 4 orders of reflections visible. At $R = 0.11$, the lamellar morphology is retained but with a reduction in *d*-spacing from 18 to 11.9 nm. This is likely due to a mesogen-driven reduction of the high interfacial tension between poly(styrene) and poly(acrylic acid) and, thus, a reduction in chain stretching away from the IMDS. This is expected given the somewhat compatibilizing nature of the mesogen, as inferred from its partial aromatic and polar structure. The domain spacing decreases with added mesogen until a plateau is reached around $R = 0.2$. Beyond this, further addition of mesogen increases the *d*-spacing, presumably by simple volumetric swelling.

A smectic bilayer structure with a layer spacing of 6.6 nm develops within the PAA domains and partially overlaps the second order reflection from the lamellar superstructure. Neither the neat diblock nor the $R = 0.11$ low stoichiometry complex display alignment on application of a 5 T magnetic field. By contrast, for $R = 0.33$ and $R = 0.40$, strongly aligned and well-ordered lamellar-within-lamellar hierarchical structures were produced on application of the 5 T field. For $R = 0.33$ and 0.40, the lamellar superstructures have *d*-spacings of 12.7 and 14 nm, respectively. The systems form monolayer smectics with layer spacings of 2 and 2.2 nm. The orientation of both the smectic substructure and block copolymer superstructures with their layer normals along the field direction is consistent with the positive diamagnetic anisotropy of the biphenyl species and its homeotropic anchoring at the IMDS of the system. The delineation of the system's response appears to coincide with

dx.doi.org/10.1021/mz2001059 | *ACS Macro Lett.* 2012, 1, 184−189

the saturation of the binding capacity of the PAA backbone for the imidazole ligand around R = 0.3, as deduced by FTIR measurements (Supporting Information).[26] Above R = 0.3, additional mesogens do not bind directly to the polymer backbone, but associate loosely with the liquid crystalline mesophase formed by already bound species. We speculate that the additional mobility afforded by the presence of these labile species aids significantly in the alignment of the system under the field. Indeed we observe that, above R = 0.3, these systems display a rich temperature-dependent phase behavior, whereas at low stoichiometries the materials are quite unresponsive to temperature, up to 180 °C. Beyond this temperature, degradation of the PAA chain occurs by anhydride formation.

A completely different scenario is presented by systems with $R \geq 0.50$. Whereas a lamellar-within-lamellar hierarchy was formed for R = 0.11, 0.33, and 0.40, a smectic LC structure surrounding hexagonally packed cylinders of PS was observed for R = 0.50, and is presumed for R = 0.80 and R = 1.0, although the absence of higher order reflections in these latter two cases did not permit unambiguous structure assignment. Figure 3 shows SAXS data for R = 0.50, 0.80, and 1.0. For R = 0.50, the system has a d-spacing of 16.9 nm in the unaligned state. After alignment, reflections along the equatorial (horizontal) line indicate that the IMDS is oriented parallel to the field direction, indicating that the cylindrical microdomains are aligned with their long axes along the field. A combination of crystalline smectic structures is present with d-spacings of 2.1 and 4.4 nm, although the large intensity at q = 0.3 Å^{-1} versus q = 0.143 Å^{-1} indicates that the 2.2 nm structures are present in large excess. The reflection at q = 0.143 Å^{-1} corresponds to a tilted monolayer while q = 0.3 Å^{-1} is due to an interdigitated tilted smectic structure. Identical structures were observed in homopolymer PAA-mesogen complexes as well.[26] Such polymorphism in side-chain LC polymers has been well documented in literature.[27,28] The LC reflections display a 4-fold symmetry and their orientation with respect to the scattering at q = 0.037 Å^{-1} indicates that the smectic layers are tilted by 25 degrees with respect to the IMDS. For R = 0.80 and 1.0, a somewhat similar situation is found, but the block copolymer superstructure displays less order and the peaks due to the microphase separated structure are significantly broadened. Analysis of the azimuthal spread of intensity for aligned materials is available in Supporting Information.

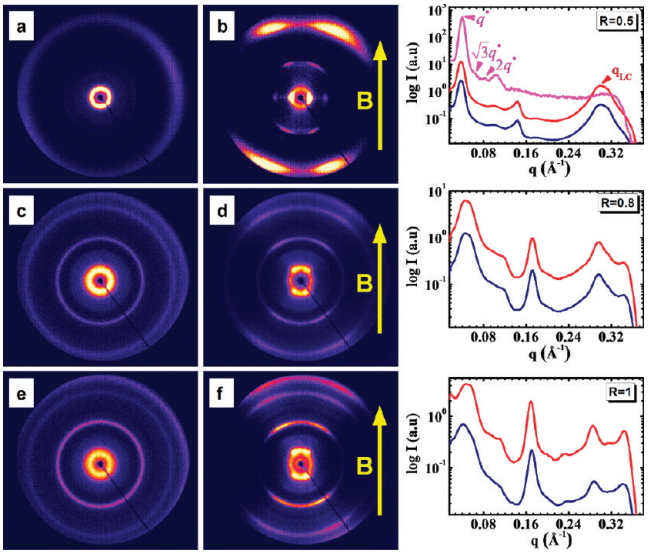

Figure 3. Room temperature 2-D SAXS and corresponding 1-D integrated data for PS-(PAA/LC)$_R$ complexes: (a) R = 0.5 (as cast); (b) R = 0.5 (after alignment); (c) R = 0.8 (as cast); (d) R = 0.8 (after alignment); (e) R = 1 (as cast), (f) R = 1 (after alignment). The field direction was vertical with respect to data, as indicated. Blue and red lines represent 1-D integrated data before and after alignment, respectively, and are vertically shifted for clarity. The magenta line for R = 0.5 data shows integrated intensity along the horizontal line where the $\sqrt{3}q^*$ and $\sqrt{4}q^*$ reflections are better resolved, indicating hexagonally packed cylinder morphology.

Real-space imaging by TEM confirms the long-range order and alignment of lamellar and cylindrical microdomains for R = 0.33 and 0.5, as inferred from the SAXS data. The lamellar interfaces are uniformly perpendicular to the field direction, whereas the cylindrical microdomains are aligned with their long axes along the field, as shown in Figure 4. Fourier transforms reveal the expected 2-fold and 6-fold symmetries of the microstructures. The change in the LC layer alignment under the field for high R systems suggests that there is a subtle concomitant change in the molecular organization of the biphenyl species that give rise to the alignment of the system. The diamagnetic anisotropy arises principally from the rigid biphenyl core and it is clear that the block copolymer superstructure is aligned expressly due to the response of these species to the field. The alignment of the biphenyl core by the field itself should not be stoichiometry dependent, and so the question arises as to how the remainder of the system is oriented around the biphenyl cores which maintain their alignment parallel to the field.

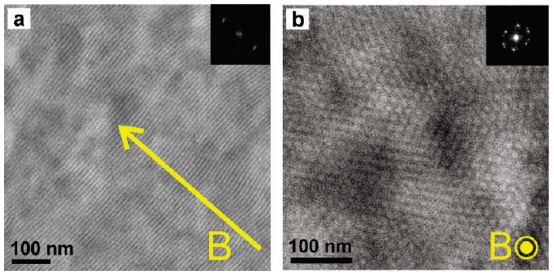

Figure 4. TEM micrographs of (a) R = 0.33 and (b) R = 0.50 samples showing lamellae and hexagonally packed cylinders, respectively. The PAA domains appear dark due to OsO_4 staining. The lamellar interfaces are aligned perpendicular to the indicated field direction whereas cylinders are aligned along the field. Insets show FFTs of the images, revealing 2-fold and 6-fold symmetries of the morphologies.

Consideration of two-dimensional WAXS data permits this to be seen in detail. Figure 5 shows 2D WAXS data from R = 0.40 and R = 0.50 samples. For R = 0.40, Figure 5a, the orthogonality of the LC layer reflection at q = 0.286 Å^{-1} and the side−side packing of the mesogens at q = 1.46 Å^{-1} (d-spacing of 0.43 nm) is clear and consistent with homeotropic anchoring of the mesogens at the IMDS, as discussed above and schematically shown in Figure 5b. Figure 5d shows data for R = 0.50. As expected, the 2-fold scattering arcs from the side−side correlations among biphenyl cores at q = 1.46 Å^{-1} are indeed still aligned orthogonal to the field, indicating that the cores are again aligned along the field direction. Strikingly, this implies that the anchoring condition of the mesogens has changed from homeotropic to planar, as depicted in Figure 5e.

dx.doi.org/10.1021/mz2001059 | ACS Macro Lett. 2012, 1, 184−189

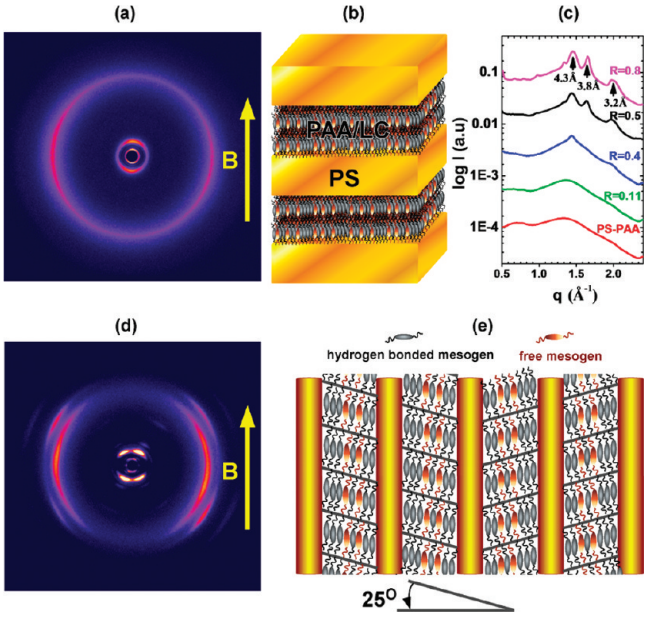

Figure 5. (a) 2-D WAXS data for R = 0.4, after alignment. Equatorial scattering at q = 1.46 Å^{-1} indicates alignment of biphenyl cores parallel to the field with 0.43 nm spacing. Lamellae and smectic layers are perpendicular to the field as in (b). (c) Integrated WAXS at room temperature at different stoichiometries. Broad scattering for R = 0.11 indicates that mesogens are loosely packed. Reflections emerge at q = 1.46 Å^{-1} on increasing R due to the increasing strength of spatial correlations among biphenyl units. For $R \geq 0.5$, a crystalline phase is formed as seen from the multiple sharp peaks. (d) 2-D WAXS for R = 0.5. The concentration of intensity on the equatorial line at q = 1.46 Å^{-1} indicates that biphenyls are parallel to the field The 4-fold symmetric scattering (d-spacing of 0.38 nm) is due to the aliphatic segments of the mesogen that are tilted with respect to the biphenyl cores. (e) Schematic illustration of alignment of cylindrical microdomains for $R \geq 0.5$. Cylinders and biphenyl cores are parallel to the field while smectic layers are tilted by about 25° relative to the surface normal of the IMDS.

In studies of covalently bonded liquid crystalline diblock copolymers to date, a strict orientational relationship has consistently been found between the LC mesophase and the block copolymer superstructure. It is this ostensibly invariant relationship that governs the response of the system to external stimuli such as magnetic fields and shear where, for example, competing alignment tendencies of the sub- and superstructure produce a compromise morphology that explicitly preserves the anchoring condition.[29] Here we observe that the anchoring condition is subject to change as a function of stoichiometry, with a resultant 90° change in the alignment of the IMDS. In Figure 5d, at q = 1.65 Å^{-1}, a 4-fold symmetric reflection is visible, corresponding to a d-spacing of 0.38 nm. This is due to correlations among the alkyl spacer and tails of the mesogen, which are clearly tilted with respect to the biphenyl core. Notably, these correlations only emerge as a function of stoichiometry for $R \geq 0.50$, Figure 5c. The picture that emerges here is that association of a large excess of unbound species with the mesophase produced by bound ligands results in a rich temperature-dependent phase behavior, crystallization of the ligands, and a change in the orientational relationship of the mesophase with respect to the block copolymer superstructure. As a result, while lamellar domains align perpendicular to the field, cylindrical domains are surprisingly found to orient parallel to the field. Both microstructures are, thus, non-degenerate. This is in stark contrast to the normal scenario where nondegenerate magnetic alignment of a lamellar system implies degeneracy in the cylindrical system and vice versa.[30] It is expressly due to the composition-dependent change in the anchoring condition of the system. This change in anchoring condition is quite intriguing. While the preferred anchoring is likely determined simply by the interaction potentials between the mesogen and the quasi-continuum IMDS, steric constraints imposed by the spacer may prevent the mesogen from adopting its preferred configuration.[31] Here, it appears that unbound mesogens facilitate the adoption of a possibly preferred planar anchoring, perhaps by screening bound mesogens from the IMDS. An alternative explanation is that the system adopts planar anchoring to avoid the s = +1 defects that must occur in an LC mesophase where mesogens are anchored homeotropically at a curved interface.[31] Additional studies of a more fundamental nature are warranted using model covalently modified side-chain LC block copolymers where mesogen dynamics are more strongly coupled to the polymer backbone by a physical instead of supramolecular connection.

Magnetic alignment represents a facile method for controlling block copolymer morphology over large length scales. The only limitation on the sample size is the lateral (and vertical) extent of the field. Polarized optical microscopy (POM) was performed to confirm uniform alignment of the system over macroscopic areas, in this case over the 0.3 mm diameter illumination of the sample, as shown in Figure 6a.

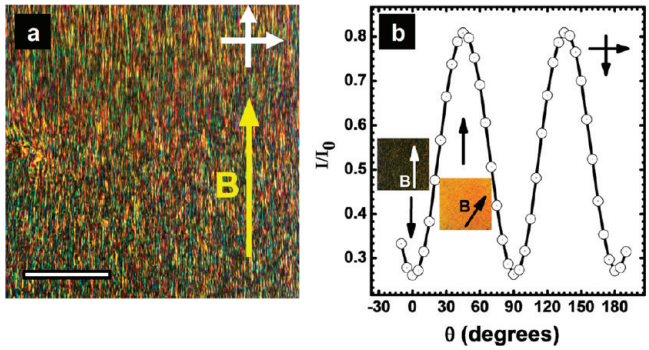

Figure 6. (a) Texture of aligned PS-(PAA/LC)$_{0.4}$ sample observed under crossed polarizers recorded at room temperature. The scale bar is 100 μm and the magnetic field direction is vertical, as indicated. (b) The transmitted light intensity normalized to the incident intensity of the aligned PS-(PAA/LC)$_{0.4}$ sample under crossed polarizers plotted against the angle (θ) between the magnetic field direction and the polarizer. The axis of rotation of the sample is parallel to the optical axis of the microscope.

Prior to alignment, random samples displayed a fine-scale grainy texture. After alignment, a banded texture was obtained as commonly observed for aligned main chain LC polymers.[32,33] The birefringence of the aligned films displayed strong optical anisotropy under crossed polarizers, Figure 6b. Periodic sinusoidal modulations in light transmission with the sample orientation are observed due to corresponding periodic variation in the smectic layer orientation relative to the plane polarization of the incident light. The smooth variation between the minima and maxima separated by 45° and the large absolute amplitude of the variation of the transmitted intensity are good indications that the system was well aligned over the large areas observed. These quantitative POM

dx.doi.org/10.1021/mz2001059 | ACS Macro Lett. 2012, 1, 184−189

measurements confirm alignment of the system over large length scales and are in good agreement with the SAXS data.

In conclusion, we have demonstrated the use of noncovalent interactions to facilitate magnetic field alignment of a self-assembled block copolymer. Hydrogen bonding between imidazole terminated biphenyl mesogens produced hierarchically ordered lamellar/lamellar and lamellar/cylinder morphologies which were strongly aligned by a 5 T field. The ability to align the system appears reliant on the mobility afforded by the presence of loosely associated ligands beyond the binding saturation capacity of the polymer backbone. The LC mesophase adopted a homeotropic anchoring at the IMDS at intermediate stoichiometries but displayed an unexpected transition to planar anchoring at high ($R \geq 0.5$) stoichiometries. These findings have important implications for the directed self-assembly of stimuli responsive supramolecular polymer systems, particularly those involving rigid chromophores and other electro-optically active species as recently advanced in literature.

EXPERIMENTAL SECTION

Materials: Poly(styrene-*b*-acrylic acid) (PS-PAA) of molecular weight 5.1 kg/mol-*b*-3.9 kg/mol (polydispersity index 1.1) was obtained from Polymer Source and used as received. The mesogenic species is based on a hydrogen bonding imidazole headgroup and a biphenyl core with 10 and 8 carbon aliphatic spacer and tail segments, respectively. Mesogen synthesis has been previously described.[26]

Sample preparation and characterization: Stock solutions of the polymer and the mesogen were separately prepared in DMF at 5 wt %. Complexes ranging from $R = 0.11$ to $R = 1$ were prepared by dropwise addition of appropriate quantities of mesogen solution to the block copolymer solution, keeping both solutions at elevated temperature (70 °C) to ensure uniform mixing. The resulting solutions were stirred at 70 °C for 1−2 h followed by solvent removal by slow evaporation at 70 °C over several hours. The resulting solid samples were annealed in vacuum at 110 °C for 24 h and then used without further treatment.

X-ray scattering: SAXS was performed on a pinhole-collimated instrument (Rigaku SMAX3000) using Cu Kα radiation (λ = 1.542 Å). The beam has a 1 mm diameter at the sample plane and the range of scattering vectors was 0.02 to 0.35 Å^{-1}. SAXS data were calibrated using a silver behenate standard. 2-D patterns were integrated azimuthally to provide 1-D representations of $I(q)$, where $q = (4\pi/\lambda) \sin \theta$, where 2θ is the scattering angle. WAXS was recorded on image plates (Fuji) and data were calibrated using silicon powder diffraction. Temperature resolved measurements were conducted using a hot stage (Linkam THMS600) with an associated temperature controller (TMS 94). Samples were subjected to a heating rate of 10 °C/min and allowed to equilibrate for 10 min at each temperature prior to data acquisition. 2-D data were rendered using WSxM.[34]

Magnetic alignment: Samples about 1−2 mm thick and 3 mm in diameter were supported on thin Kapton windows on a temperature controlled aluminum stage within a superconducting magnet (American Magnetics Inc.) at a flux density of 5 T. The samples were heated to 170 °C and then allowed to cool at 4 °C/min to room temperature in the presence of the field.

DSC and POM: DSC was performed using a TA Instruments Q200 with a heating rate of 20 °C/min. Aligned samples were examined optically using a Zeiss Axiovert 200 M microscope equipped with a Pike CCD camera. For POM, samples were confined between two glass slides with a thin PTFE tape used as a spacer. Measurements were made in transmission under crossed polarizers at 20× magnification.

TEM: Thin sections of 50−100 nm thickness were prepared by ultramicrotoming using a diamond knife. Sections were collected on TEM grids after flotation onto water and stained in OsO4 vapor for 30 min prior to imaging. Bright-field microscopy was performed using a FEI Tecnai BioTwin instrument with an accelerating voltage of 120 kV. Images were edited and rendered with WSxM.[34]

ASSOCIATED CONTENT

Supporting Information

FTIR spectra and DSC of block copolymer complexes. This material is available free of charge via the Internet at http://pubs.acs.org.

AUTHOR INFORMATION

Corresponding Author

*E-mail: chinedum.osuji@yale.edu.

Notes

The authors declare no competing financial interest.

ACKNOWLEDGMENTS

The authors gratefully acknowledge funding from NSF via DMR-0847534 (P.M., M.G., and C.O.). The authors thank American Magnetics Inc. for their technical support. Kind assistance in sample preparation and microtomy for TEM from Ms. Morven Graham of Yale SOM and Dr. Barry Piekos of Yale MCDB is also acknowledged.

REFERENCES

(1) Brunsveld, L.; Folmer, B. J. B.; Meijer, E. W.; Sijbesma, R. P. *Chem. Rev.* **2001**, *101* (12), 4098.
(2) Kawakami, T.; Kato, T. *Macromolecules* **1998**, *31* (14), 4475.
(3) Kato, T. Hydrogen-Bonded Liquid Crystals: Molecular Self-Assembly for Dynamically Functional Materials. In *Structure and Bonding*; Springer: Berlin/Heidelberg, 2000; Vol. *96*, pp 95−146.
(4) ten Brinke, G.; Ruokolainen, J.; Ikkala, O. Supramolecular Materials Based on Hydrogen-Bonded Polymers. In *Hydrogen Bonded Polymers*; Springer-Verlag: Berlin Heidelberg, 2007; Vol. *207*, pp 113−177.
(5) Kato, T.; Frechet, J. M. J. *Macromol. Symp.* **1995**, *98*, 311−326.
(6) Zhao, Y.; Thorkelsson, K.; Mastroianni, A. J.; Schilling, T.; Luther, J. M.; Rancatore, B. J.; Matsunaga, K.; Jinnai, H.; Wu, Y.; Poulsen, D.; Frechet, J. M. J.; Paul Alivisatos, A.; Xu, T. *Nat. Mater.* **2009**, *8* (12), 979.
(7) Ruokolainen, J.; Makinen, R.; Torkkeli, M.; Makela, T.; Serimaa, R.; ten Brinke, G.; Ikkala, O. *Science* **1998**, *280* (5363), 557−560.
(8) Kosonen, H.; Ruokolainen, J.; Knaapila, M.; Torkkeli, M.; Jokela, K.; Serimaa, R.; ten Brinke, G.; Bras, W.; Monkman, A. P.; Ikkala, O. *Macromolecules* **2000**, *33* (23), 8671−8675.
(9) Osuji, C.; Chao, C. Y.; Bita, I.; Ober, C. K.; Thomas, E. L. *Adv. Funct. Mater.* **2002**, *12* (11−12), 753−758.
(10) Valkama, S.; Kosonen, H.; Ruokolainen, J.; Haatainen, T.; Torkkeli, M.; Serimaa, R.; Ten Brinke, G.; Ikkala, O. *Nat. Mater.* **2004**, *3* (12), 872−876.
(11) Rancatore, B. J.; Mauldin, C. E.; Tung, S.-H.; Wang, C.; Hexemer, A.; Strzalka, J.; Frechet, J. M. J.; Xu, T. *ACS Nano* **2010**, *4* (5), 2729.
(12) Sary, N.; Richard, F.; Brochon, C.; Leclerc, N.; Lévêque, P.; Audinot, J.-N.; Berson, S.; Heiser, T.; Hadziioannou, G.; Mezzenga, R. *Adv. Mater.* **2010**, *22* (6), 763.
(13) Hsu, J.-C.; Liu, C.-L.; Chen, W.-C.; Sugiyama, K.; Hirao, A. *Macromol. Rapid Commun.* **2011**, *32* (6), 528.
(14) Darling, S. B. *Prog. Polym. Sci.* **2007**, *32* (10), 1204.
(15) Sun, H.-S.; Lee, C.-H.; Lai, C.-S.; Chen, H.-L.; Tung, S.-H.; Chen, W.-C. *Soft Matter* **2011**, *7* (9), 4206.
(16) Kauranen, M.; Verbiest, T.; Boutton, C.; Teerenstra, M. N.; Clays, K.; Schouten, A. J.; Nolte, R. J. M.; Persoons, A. *Science* **1995**, *270* (5238), 969.
(17) Osuji, C.; Ferreira, P. J.; Mao, G. P.; Ober, C. K.; Vander Sande, J. B.; Thomas, E. L. *Macromolecules* **2004**, *37* (26), 9903−9908.
(18) Lasheen, M. A. *Philos. Trans. R. Soc., A* **1964**, *256* (1073), 387.

(19) Charbonneau, G. P.; Rivet, P. *Acta Crystallogr., Sect. A* **1980**, *36* (JAN), 51−53.
(20) Gopinadhan, M.; Majewski, P. W.; Osuji, C. O. *Macromolecules* **2010**, *43* (7), 3286−3293.
(21) Majewski, P. W.; Gopinadhan, M.; Jang, W.-S.; Lutkenhaus, J. L.; Osuji, C. O. *J. Am. Chem. Soc.* **2010**, *132* (49), 17522.
(22) Tao, Y.; Zohar, H.; Olsen, B. D.; Segalman, R. A. *Nano Lett.* **2007**, *7* (9), 2746.
(23) Majewski, P. W.; Gopinadhan, M.; Osuji, C. O. *J. Polym. Sci., Part B: Polym. Phys.* **2011**, DOI: 10.1002/polb.22382.
(24) Xu, B.; Pinol, R.; Nono-Djamen, M.; Pensec, S.; Keller, P.; Albouy, P.-A.; Levy, D.; Li, M.-H. *Faraday Discuss.* **2009**, *143*, 235.
(25) Osuji, C. O.; Chao, C.-Y.; Ober, C. K.; Thomas, E. L. *Macromolecules* **2006**, *39* (9), 3117.
(26) Gopinadhan, M.; Beach, E. S.; Anastas, P. T.; Osuji, C. O. *Macromolecules* **2010**, *43* (16), 6646−6654.
(27) Saez, I. M.; Goodby, J. W. Supermolecular Liquid Crystals. In *Liquid Crystalline Functional Assemblies And Their Supramolecular Structures*; Springer-Verlag: Berlin, 2008; Vol. *128*, pp 1−62.
(28) Yamaguchi, T.; Asada, T.; Hayashi, H.; Nakamura, N. *Macromolecules* **1989**, *22* (3), 1141−1144.
(29) Osuji, C.; Zhang, Y. M.; Mao, G. P.; Ober, C. K.; Thomas, E. L. *Macromolecules* **1999**, *32* (22), 7703−7706.
(30) Majewski, P. W.; Osuji, C. O. *Soft Matter* **2009**, *5* (18), 3417−3421.
(31) Osuji, C. O.; Chen, J. T.; Mao, G.; Ober, C. K.; Thomas, E. L. *Polymer* **2000**, *41* (25), 8897.
(32) Pardey, R.; Shen, D.; Gabori, P. A.; Harris, F. W.; Cheng, S. Z. D.; Adduci, J.; Facinelli, J. V.; Lenz, R. W. *Macromolecules* **1993**, *26* (14), 3697.
(33) Kiss, G.; Porter, R. S. *Mol. Cryst. Liq. Cryst.* **1980**, *60* (4), 267−&.
(34) Horcas, I.; Fernandez, R.; Gomez-Rodriguez, J. M.; Colchero, J.; Gomez-Herrero, J.; Baro, A. M. *Rev. Sci. Instrum.* **2007**, *78* (1), 013705.